Contact Stiffness Governs Mechanoresponses of Living Cells to Extracellular Microenvironment

Peng Zhao[1,2,#], Yang Zheng[1,#], Zhao-Yi Zhang[1], Ming-Wei Jiang[1], Yu-Xuan Jiang[1], Jing Du[2,*], Yanping Cao[1,*]

[1]Institute of Biomechanics and Medical Engineering, AML, Department of Engineering Mechanics, Tsinghua University, Beijing 100084, China.

[2]Key Laboratory of Biomechanics and Mechanobiology (Beihang University), Ministry of Education, Beijing Advanced Innovation Center for Biomedical Engineering, School of Biological Science and Medical Engineering, Beihang University, Beijing, 100083, China.

[†] Co-first authors with equal contribution.

* Corresponding authors: caoyanping@tsinghua.edu.cn (Y.P..C); dujing@buaa.edu.cn (J.D.)

ABSTRACT

Extracellular microenvironment properties (including physical, chemical and geometrical aspects) have profound effects on the fate of living cells. However, the interplay underlying these regulations remains unclear. Based on the fact that interaction of living cells with extracellular matrix (ECM) is a typical contact problem, we proposed a contact stiffness (CS)-based model to address cell mechanoresponses. Our model provides a unified means to address the effect of physical parameters e.g. intrinsic ECM stiffness and geometrical factors including ECM thickness and cell spreading area on cell behaviors, such as stem cell differentiation and YAP activation in different experimental conditions. We show that the CS for living cells contact with ECM is not merely a passive variable but can be actively tuned by cell itself, and thus help understand the response of cells to non-adjacent layer of layered ECM. We also reveal that the broad variation range of CS is an intrinsic characteristic of a certain cell type which reflects its "mechanical plasticity" in response to extracellular microenvironment.

INTRODUCTION

Mammalian cells contact with neighboring cells and extracellular matrix (ECM) and are sensitive to mechanical cues from surrounding microenvironment. Numerous studies have addressed the critical roles played by intrinsic stiffness of ECM and the cell geometry including spreading area in cell mechanosensitivity[1-5]; however, the interplay between the physical stimuli and geometrical factors remains unknown. The interaction of living cells with ECM is a typical contact problem. In contact mechanics theory [6], contact stiffness (CS) is a key variable defining how physical and geometrical parameters (e.g., elastic moduli, contact geometry and thickness of layered contact solids) determine the variation of contact load with contact deformation[7,8] .

Considering the essential role of CS in contact interaction of solids, we investigate its effect on the fate of living cells for the first time. Taking YAP activity and stem cell differentiation as typical examples, we show that introduction of the concept of CS enables a unified analysis of the influences of intrinsic stiffness of ECM depending on its constitutive laws and geometric parameters including thickness of ECM and cell spreading area. A scaling relation between YAP activation and CS is uncovered. Remarkably, CS is not merely a passive variable relying on the physical and geometrical parameters of ECM, but can be actively modulated by cell itself through changing its geometry and spread area. Therefore, the proposed CS-based model also provides the opportunity to reveal the connections among chemical signals, physical stimuli and geometric parameters of the cell-ECM system in tuning cell mechanoresponses.

RESULTS

Contact stiffness incorporates ECM intrinsic stiffness, thickness, cell geometry and spreading area

In living organisms, cells contact with ECM and are continuously exposed to physical forces imposed by surrounding microenvironment and they respond by modulating their behaviours and generating their own forces[9,10]. In view the interaction between living cells and ECM is a typical contact problem, here we address the interaction of cells with the ECM and their diverse mechnosensing behaviours by proposing a CS-based model. CS is a fundamental variable in the theory of contact mechanics, which defines the correlation of contact deformation with interaction force. CS is given by $S = C_0 E^* \sqrt{A}$ (see SI1 for details) based on Sneddon's solution[11] for a thick ECM. where C_0 is a constant, E^* is the equivalent elastic modulus and A is the contact area (cell spreading area). In this paper, the ECM deformation and its reaction force to the cell are the main concern and E^* represents the intrinsic ECM stiffness. If the thickness of ECM has to be considered (i.e., ECM is thin and comparable with the dimension of cells), the CS is given by $S = E^* \sqrt{A} \Pi\left(\sqrt{A}/t\right)$, where Π is a dimensionless function[12] and t is the ECM thickness. When the cell geometry (and also the contact geometry) is far from axisymmetric, it affects the CS as well and a correction factor based on cell geometry may be introduced as suggested by our finite element analysis (Supplementary Figure S1). Therefore, the CS incorporates ECM intrinsic stiffness and geometrical parameters e.g., ECM thickness, cell geometry and spreading area and may play a more fundamental role in cell responses to the microenvironment.

To address how the CS affects cell mechanoresponses, we cultured MSCs on a layered substrate composed of polyacrylamide (PA) gel with gradient thickness on a glass slip which leads to a continuous gradient of contact stiffness (Figure 1a). The spreading area of cells decreased as the thickness of PA gel increased (i.e., from 1000 μm^2 on a gel with the thickness of 174 μm to around 16000 μm^2 on a gel with the

thickness of 6 μm , the gel modulus in both cases is 100 kPa) (Figure 1b and 1c). By measuring the physical and geometrical parameters of the system and according to the definition of the CS as shown above, we can calculate the CS as a function of gel thickness (i.e., from 8 N/m for the gel with thickness of 174 μm to 547 N/m for the gel with thickness of 6 μm thickness, the gel modulus in both cases is 100 kPa) (Figure 1d).

By modulating the modulus of PA gels (0.5 kPa, 10 kPa, 40 kPa and 100 kPa) (Figure 1e), the magnitude of the CS spanned over five orders (from 0.012 to 547 N/m), that is approximately 3-orders more than the variation rang of gel intrinsic stiffness (from 0.5 to 100 kPa) (Figure 1g). The definition and calculation of the CS show that it not only depends on the passive parameters e.g., ECM intrinsic stiffness and thickness, but also can be actively tuned by cell itself by changing its geometry and spreading area (Figure 1f) and may have a broad range of variation.

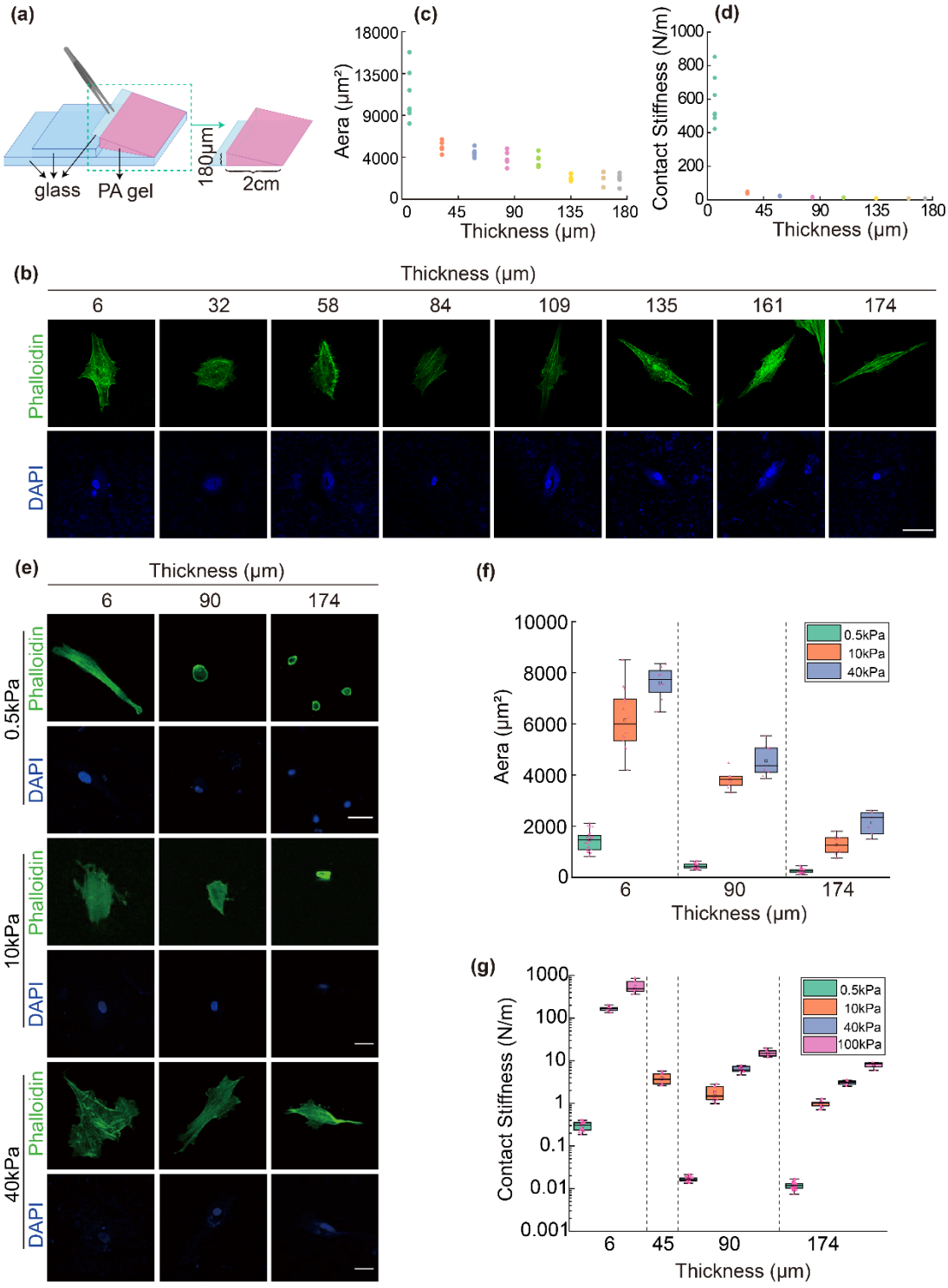

Figure 1. MSCs cultured on PA hydrogels with gradient contact stiffness (a) Illustration of the fabrication process of PA hydrogels with gradient thickness. **(b)** Representative images of F-actin and nucleus in MSCs on 100 kPa hydrogels with gradient thickness stained by phalloidin (green) and DAPI (bule) , respectively. Scale bar: 75 μm. **(c)** Spreading area of MSCs on PA hydrogel with gradient thickness for the results in (b). **(d)** Contact stiffness of MSCs on PA hydrogel with gradient thickness for the results in (b). **(e)** Representative images of F-actin and nucleus in MSCs on 0.5kPa, 10 kPa and 40 kPa PA hydrogels with greadient thickness stained by phalloidin (green) and DAPI

(bule) , respectively. Scale bar: 50 μm. **(f)** Statistical analysis of cell spreading area of MSCs on PA hydrogel with different stiffness and thickness. **(g)** Statistical analysis of contact stiffness of MSCs on PA hydrogel with different stiffness and thickness.

Contact stiffness plays a key role in directing stem cell differentiation

The pivotal function of physical microenvironment in directing stem cell lineage specification has been extensively studied[2,13] and ECM with different mechanical properties has been frequently used. To explore the regulation of MSCs differentiation by contact stiffness, we altered the CS by changing geometrical parameters i.e., ECM thickness[14] with the ECM elastic properties unchanged. It should be pointed out that modulating the ECM geometry can be much easier than tuning its physical parameters; moreover, changing the former does not alter the chemical properties and microstructures of the ECM.

Our results show that the expression levels of osteogenesis markers (Runx2 and Collagen I) significantly increased with the increase in the CS, especially when the CS was over 1 N/m (Figure 2a-d). Whereas the expression levels of neurogenesis markers (NF-68kD and Nestin) decreased with the increase in CS when it was less than 1 N/m. However, when the CS was over 10 N/m, the expression of neurogenetic markers were basically not affected by the CS (Figure 2e-h). These results demonstrate the profound effect of the CS on stem cell differentiation. It should be pointed out that a cell alters its spreading area on gels with different thickness as shown in Figure 1c and 1f, and this information has been included in the calculation of the CS. Previous studies have demonstrated that cell spreading area depends on the activity of adhesion molecules (focal adhesions (FAs)) and actin filaments (F-actin)[15,16]. In this study, we also examined correlation of the assembly of FAs with the CS. The results showed an increase tendency in FAs assemblies with increase in CS (Supplementary Figure S2). Given the dynamic variation of CS in cell mechanosensing, we proceed to investigate how a living cell tune the CS in its interaction with microenvironment.

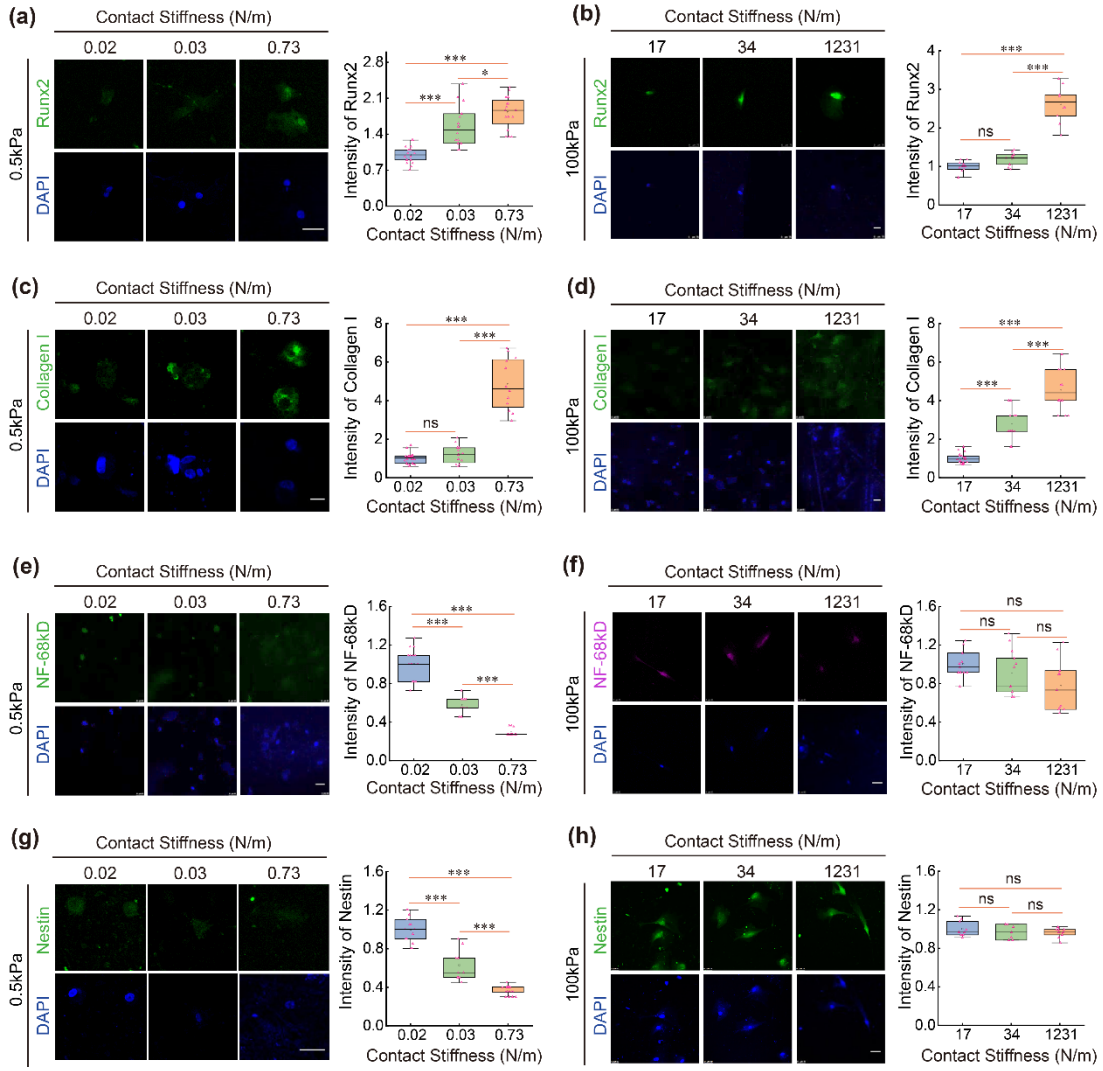

Figure 2 Contact stiffness regulates MSCs differentiation (a) (Left) Representative images of RUNX2 expression and nucleus in MSCs cultured on 0.5 kPa PA hydrogel with different contact stiffness for 4 days stained by RUNX2 antibody (green) and DAPI (blue), respectively. Scale bar: 50 μm. (Right) The statistical analysis of RUNX2 expression level in MSCs cultured on 0.5 kPa PA hydrogel with different contact stiffness for 4 days. **(b)** (Left) Representative images of RUNX2 expression and nucleus in MSCs cultured on 100 kPa PA hydrogel with different contact stiffness for 4 days stained by RUNX2 antibody (green) and DAPI (blue), respectively. Scale bar: 50 μm. (Right) The statistical analysis of RUNX2 expression level in MSCs cultured on 100 kPa PA hydrogel with different contact stiffness for 4 days. **(c)** (Left) Representative images of Collagen I expression and nucleus in MSCs cultured on 0.5 kPa PA hydrogel with different contact stiffness for 4 days stained by Collagen I antibody (green) and DAPI (blue), respectively. Scale bar: 50 μm. (Right) The statistical analysis of Collagen I expression level in MSCs cultured on 0.5 kPa PA hydrogel with different contact stiffness for 4 days. **(d)** (Left) Representative images of Collagen I expression and nucleus in MSCs cultured on 100 kPa PA hydrogel with different contact stiffness for 4 days stained by Collagen I antibody (green) and DAPI (blue), respectively. Scale bar: 50 μm. (Right) The statistical analysis of Collagen I expression level in MSCs cultured on 0.5 kPa PA hydrogel with different contact stiffness for 4 days. **(e)** (Left) Representative images of NF-68kD

expression and nucleus in MSCs cultured on 0.5 kPa PA hydrogel with different contact stiffness for 4 days stained by NF-68kD antibody (green) and DAPI (blue), respectively. Scale bar: 50 μm. (Right) The statistical analysis of NF-68kD expression level in MSCs cultured on 0.5 kPa PA hydrogel with different contact stiffness for 4 days. **(f)** (Left) Representative images of NF-68kD expression and nucleus in MSCs cultured on 100 kPa PA hydrogel with different contact stiffness for 4 days stained by NF-68kD antibody (green) and DAPI (blue), respectively. Scale bar: 50 μm. (Right) The statistical analysis of Collagen I expression level in MSCs cultured on 0.5 kPa PA hydrogel with different contact stiffness for 4 days. **(g)** (Left) Representative images of Nestin expression and nucleus in MSCs cultured on 0.5 kPa PA hydrogel with different contact stiffness for 4 days stained by Nestin antibody (green) and DAPI (blue), respectively. Scale bar: 50 μm. (Right) The statistical analysis of Nestin expression level in MSCs cultured on 0.5 kPa PA hydrogel with different contact stiffness for 4 days. **(h)** (Left) Representative images of Nestin expression and nucleus in MSCs cultured on 100 kPa PA hydrogel with different contact stiffness for 4 days stained by Nestin antibody (green) and DAPI (blue), respectively. Scale bar: 50 μm. (Right) The statistical analysis of Collagen I expression level in MSCs cultured on 0.5 kPa PA hydrogel with different contact stiffness for 4 days. *P < 0.05, **P < 0.01, ***P < 0.001. ns: not statistically significant.

Contact stiffness can be actively tuned by the mechanical plasticity of living cells in response to the microenvironment

Stem cell differentiation is a progressive process involving genetic alterations over time. Interestingly, by comparing MSCs in distinct time points during differentiation induced by ECM stiffness and thickness, we found a significant increase tendency of cell spreading area from Day1 to Day4 (Figure 3). Consequently, the contact stiffness also increased over time (Figure 3c and 3f), which may in turn contribute to stem cell differentiation.

By comparing the CS of different cell types in the same microenvironment, we found that the variation range of CS is quite different in different cell types (Figure 3g). Interestingly, the variation range of stem cells in the CS is the widest in comparison with other differentiated cells (Figure 3g). These results suggest that the CS provides a new point of view to understand the common mechanism underlying cell spatiotemporal responses to external stimuli as it can be actively tuned by cell itself.

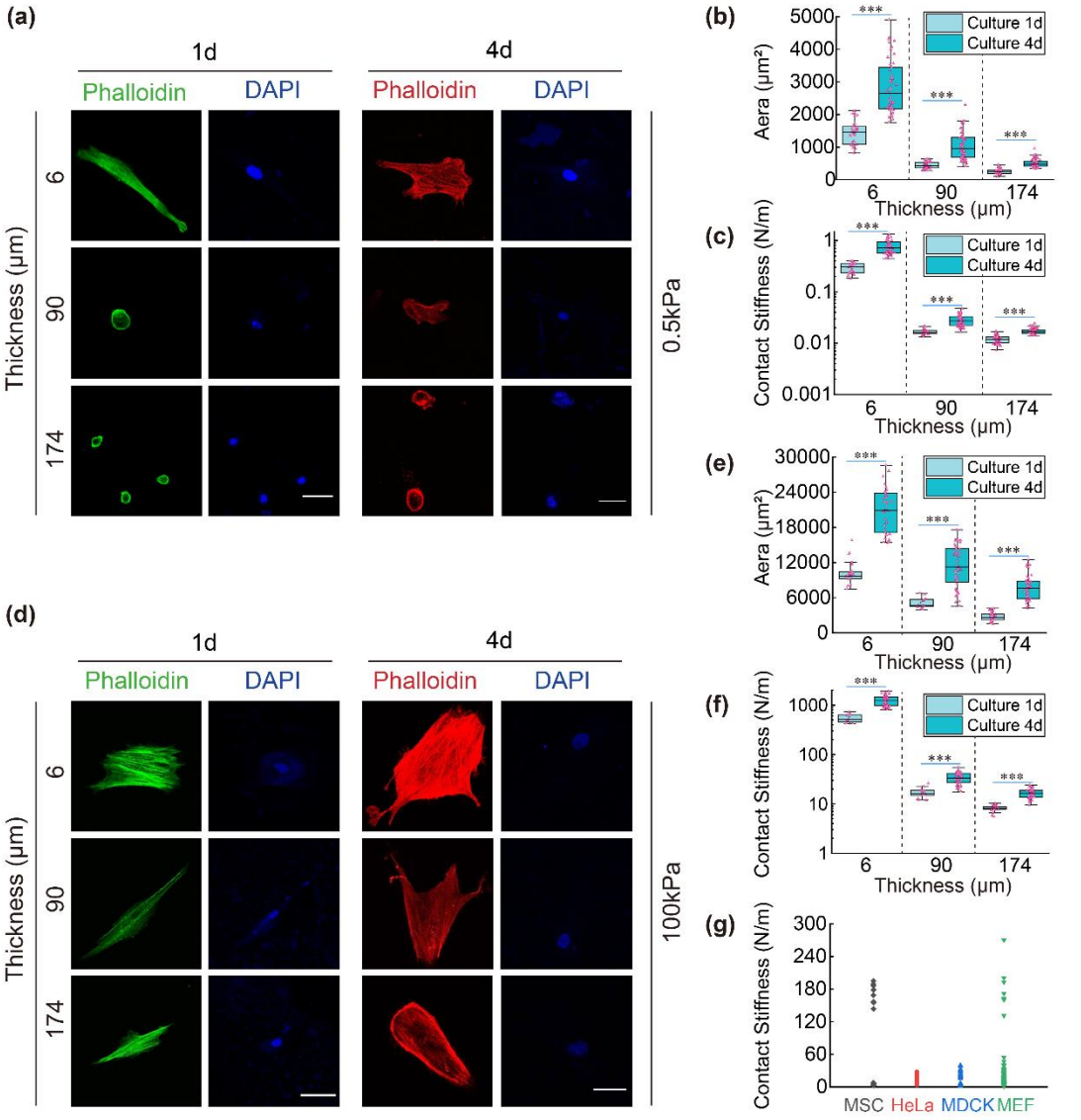

Figure 3 Contact stiffness can be actively tuned by the mechanical plasticity of living cells in response to the microenvironment (a) Representative cell images of F-actin and nucleus in MSCs cultured on 0.5 kPa PA hydrogels with gradient thickness for 1 or 4 days stained by phalloidin and DAPI, respectively. Scale bar: 50 μm. **(b)** The statistical analysis of cell spreading of MSCs cultured on 0.5 kPa PA hydrogels with gradient thickness for 1 or 4 days. **(c)** The statistical analysis of contact stiffness of MSCs cultured on 0.5 kPa PA hydrogels with gradient thickness for 1 or 4 days. **(d)** Representative cell images of F-actin and nucleus in MSCs cultured on 100 kPa PA hydrogels with gradient thickness for 1 or 4 days stained by phalloidin and DAPI, respectively. Scale bar: 50 μm. **(e)** The statistical analysis of cell spreading of MSCs cultured on 100 kPa PA hydrogels with gradient thickness for 1 or 4 days. **(f)** The statistical analysis of contact stiffness of MSCs cultured on 0.5 kPa PA hydrogels with gradient thickness for 1 or 4 days. **(g)** The statistical analysis of CS of MSCs, HeLa, MDCK and MEF cultured on 40 kPa PA hydrogels with different contact stiffness. *P < 0.05, **P < 0.01, ***P < 0.001.

A scaling relation between contact stiffness with YAP activity

Emerging evidences have demonstrated the mechanical sensing function of cell nucleus [17,18], here we proceed to investigate the response of cell nucleus to the CS. We first assessed the assembly of nuclear lamina by immunostaining of the major protein Lamin A/C[19,20]. The results showed that the intensity of Lamin A/C was coordinated with the CS (Supplementary Figure S3).

As a transcriptional factor, Yet-associated Protein (YAP) plays important roles in embryonic development, tissue growth, etc.[17,21]. Moreover, numerous studies demonstrate that mechanical stimuli have profound effect on the activity of YAP indicated by its nuclear/cytoplasmic distribution (N/C ratio) [22]. We found that the N/C ratio of YAP was continuously increased with the increase of the CS (Figure 4). By combining the gels with different moduli of 10 kPa, 40 kPa, and 100 kPa, the CS will span four orders (from 0.1~1000 N/m). Remarkably, we found for gels with different intrinsic stiffness, when the CS was comparable, YAP N/C ratio was similar (Figure 4c and 4e). To confirm the dominant effect of the CS, we modulated contact stiffness by disrupting the assembly of F-actin through chemical treatment (Cytochalasin) and also found a coordinating variation tendency of YAP N/C ratio value with contact stiffness (Figure 4d). This indicates that the CS-based model may help reveal the mechanosensing mechanism of living cells subject to chemical treatment. Interestingly, when combining all of the data of cells in different physical and chemical microenvironment, CS scales well with YAP N/C ratio in the form of a power function (Figure 4e).

In previous studies, effects of ECM intrinsic stiffness (determined by its mechanical properties) and geometrical factors e.g., cell spreading area on cell behaviors have been addressed separately. In our CS-based model, their effects can be unified by introducing the CS as a control variable. To confirm this conclusion, we also examined the data set in the literature. We extracted the experimental data from previous studies [23-24] and calculated the contact stiffness according to the cell spreading area and stiffness of substrate (Supplementary Figure S4). By analyzing the correlation

of YAP N/C ratio and the CS, we found a scaling relationship between these two parameters (Supplementary Figure S4). These results indicate that YAP activity universally scales well with the CS in response to different microenvironment.

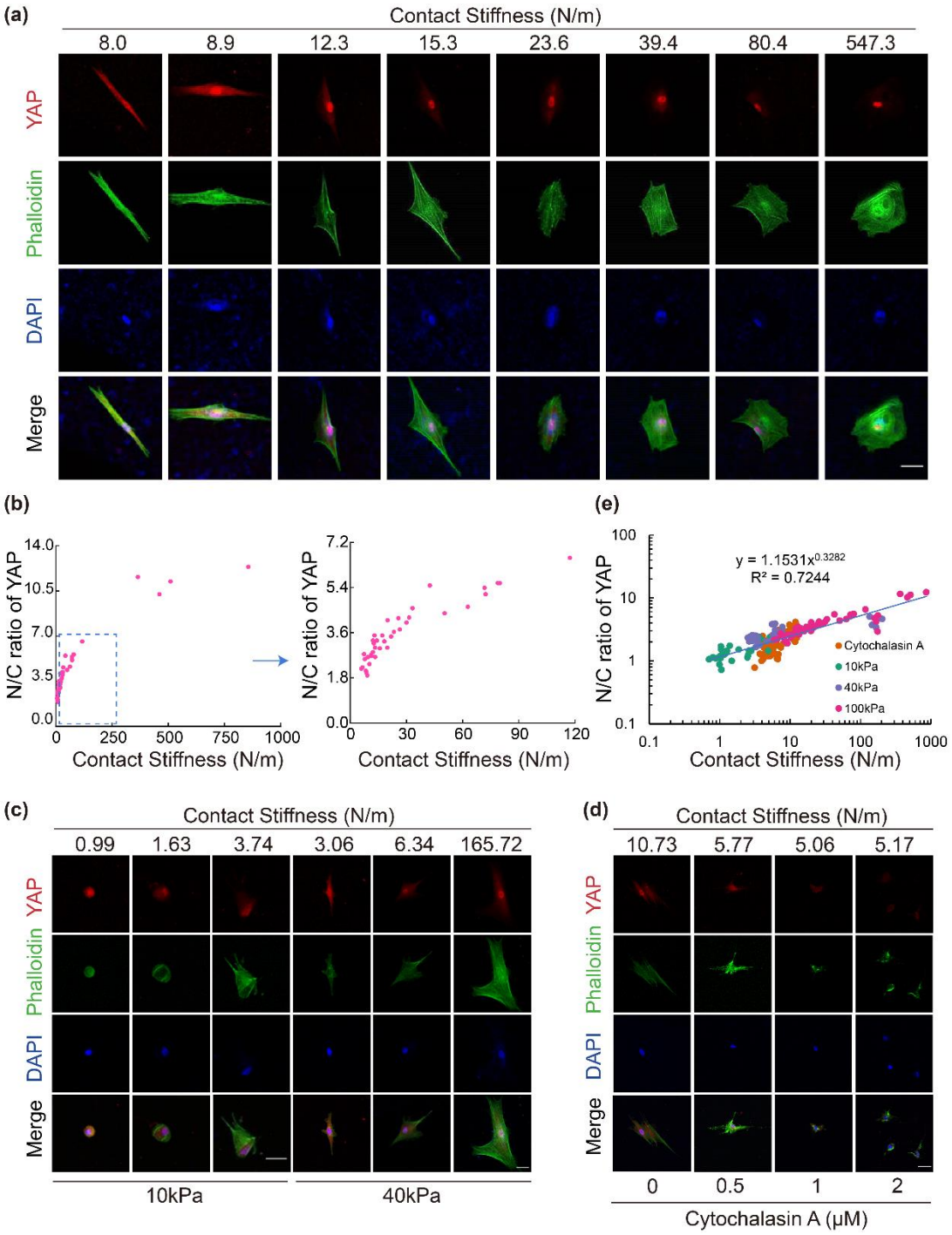

Figure 4 A scaling relation between contact stiffness and YAP nuclear/cytoplasmic ratio. (a) Representative images of YAP, F-actin and nucleus in MSCs cultured on 100 kpa PA hydrogels at different contact stiffness stained by YAP antibody (red), phalloidin (green) and DAPI (blue),

respectively. Scale bar: 75 μm. **(b)** Scatter plot of YAP nuclear/cytoplasmic ratio at different contact stiffness in (a). **(c)** Representative images of YAP, F-actin and nucleus in MSCs cultured on 10 kPa or 100 kpa PA hydrogels at different contact stiffness stained by YAP antibody (red), phalloidin (green) and DAPI (blue), respectively. Scale bar: 75 μm. **(d)** Representative images of YAP, F-actin and nucleus in MSCs cultured on 100 kpa PA hydrogels treated with Cytochalasin A at different concentrations stained by YAP antibody (red), phalloidin (green) and DAPI (blue), respectively. Scale bar: 50 μm. **(e)** Scatter plot of YAP nuclear/cytoplasmic ratio at different contact stiffness in MSCs cultured on 10 kpa, 40 kpa, 100 kpa gradient hydrogels or treated with Cytochalasin A.

DISCUSSION

The interaction of living cells with surrounding microenvironment may be tuned by chemical, physical and geometrical factors as addressed in previous studies [25-27]. In contact theory[6] , the contact stiffness defines the relationship between the deformation and the reaction force of ECM to a living cell, which inspires us to propose a CS-based model to address the interplay among chemical, physical and geometrical factors involved in cell mechanoresponses. CS has clear physical meaning and incorporates physical parameters e.g., ECM intrinsic stiffness and ECM thickness, and geometrical parameters including cell geometry and spreading area into one variable. Some chemical treatments may alter cell geometry and spreading area and its effect may be represented with the CS as well. Variation of the spreading area is accompanied by the change of the total amount of focal adhesion and cell geometry determines the distribution of focal adhesion (Supplementary Figure S2). In this sense, the dynamic variation in the focal adhesion including its amount and the way of distribution caused by physical, geometrical or chemical factors leads to a dynamic change in the CS according to our model, and alters the interaction of cells with the ECM.

In live organisms, the ECM is not a homogeneous material and may be in the form of a layered composite. Our CS-based model enables revealing the effect of non-adjacent layers. In a previous study, Chen and co-authors investigated a layered ECM, they used the apparent elastic modulus given by indentation to describe ECM stiffness and addressed its effect on cell migration behaviors[28] . According to the experiments in our present work, the *non-adjacent layer* of layered ECM (we called supra-substrate) may not only change the equivalent modulus of the ECM but also later the cell

spreading area in regulating cell behaviors; all these factors will affect the interaction between the ECM and cells and can be predicted by our CS-based model. To further demonstrate the use of our theory in understanding the effect of non-adjacent layer, we altered the elastic moduli of different layers with 10 kPa gel as the top layer and 40 or 100 kPa gel as the bottom layer (Figure 5a). Cell spreading area increased with the increase in intrinsic stiffness of supra-substrate (Figure 5b and 5c), which leads to a greater CS according to our model (Figure 5d). Moreover, stiffer supra-substrate causes a greater YAP N/C ratio (Figure 5e and 5f). Importantly, similar YAP N/C ratio was observed in different supra-substrate gels whereas the CS was comparable (i.e., 0.93 N/m in 10/40 kPa gel and 1.12 N/m in 10/100 kPa gel). These results indicate that non-adjacent layers may regulate cell behaviors through altering the CS of the composite system.

Collective cell migration has received considerable attention due to its essential role in morphogenesis and tissue remodelling. In a recent study[29], the importance of mechanical cues in the collective migration of the Xenopus laevis neural crest cells has been revealed. It was shown that that mesoderm stiffening is necessary and sufficient to trigger neural crest migration. Remarkably, a link between two apparently unconnected processes—gastrulation and neural crest migration has been uncovered considering changes in tissue mechanics. In view the essential role played by the CS in understanding the interaction of living cells with surrounding microenvironment, investigation of its effect on the collective migration of cells in coordinating morphogenesis and cancer invasion is important and deserves further effort.

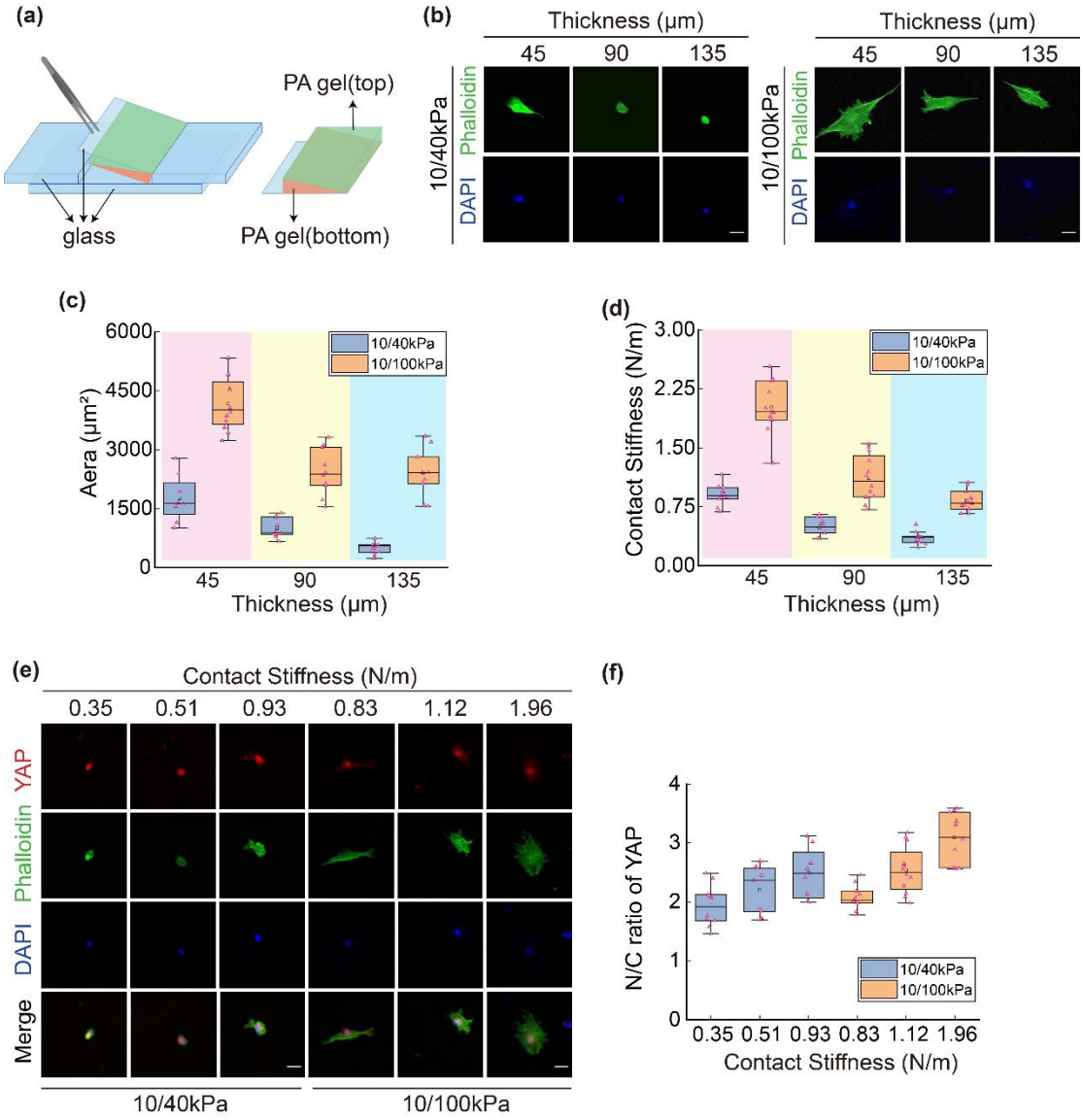

Figure 5 The nonadjacent layer of ECM regulates the YAP activity through affecting contact stiffness (a) Illustration of the fabrication process of two-layered PA hydrogels with gradient thickness. **(b)** Representative images of F-actin and nucleus in MSCs on two-layered hydrogels (10/40 kPa: bottom 40 kpa, top 10 kpa; 10/100 kPa: bottom 100 kpa, top 10 kpa) with gradient thickness stained by phalloidin (green) and DAPI (bule) , respectively. Scale bar: 50 μm. **(c)** Spreading area of MSCs on two-layered PA hydrogel with gradient thickness for the results in (b). **(d)** Contact stiffness of MSCs on two-layered PA hydrogel with gradient thickness for the results in (b). **(e)** Representative images of YAP, F-actin and nucleus in MSCs cultured on two-layered PA hydrogels at different contact stiffness stained by YAP antibody (red), phalloidin (green) and DAPI (blue), respectively. Scale bar: 50 μm. **(f)** Statistical analysis of YAP nuclear/cytoplasmic ratio at different contact stiffness in (e).

ACKNOWLEDGEMENT

This study was supported by the National Natural Science Foundation of China (NSFC) (11972206, 11572179, 11432008, 12222201), the National Key R&D Program of China (2017YFA0506500) and Fundamental Research Funds for the Central Universities (ZG140S1971). **Contributions:** Y.P.C. suggested the CS-based model, J.D. and Y.P.C. designed and supervised the experiments, P.Z., Y.Z. and Y.X.J performed the experiments, Z.Y.Z. and M.W.J. developed the finite element model. All the authors took part in the data analysis. J.D. and Y.P.C. wrote the paper.

METHOD

Fabrication of PA hydrogels with gradient thickness

Single layer PA hydrogel molds were fabricated with one 70- × 24- × 1-mm glass slide (CITOTEST) and one 24- × 24- × 0.18 mm (CITOTEST) forming the mold. (Fig. 1a). Double layer hydrogel molds were fabricated with one 70- × 24- × 1-mm glass slide (CITOTEST) and two 24- × 24- × 0.18 mm (CITOTEST) (Fig. 5a).

PA hydrogel preparation was performed according to J. Engler et al [30]. The mixed liquid cover glass liquid was added to the mold. Use 3 suitable clips to clip the ends of the functionalized wave plate and the base wave plate. After polymerization, single layer PA hydrogel was removed from the mold and placed into a 6-well plate with PBS and stored in a 4°C refrigerator. Double layer PA hydrogels which prepared single-layer PA hydrogel was inverted in the mold. the mixed liquid cover glass liquid was added to the mold. After polymerization, the sample was removed from the mold and placed into a 6-well plate with PBS and stored in a 4°C refrigerator. The prepared PA hydrogel was functionalized according to the method described above [30].

Cell Culture

MSCs, HeLa, MDCK and MEFs were cultured in dulbecco's modified eagle medium (DMEM) medium (containing with 4.5 g L^{-1} glucose, l-glutamine, and sodium pyruvate) supplemented with 10% fetal bovine serum (FBS; Life technologies, CA, USA), and

100 IU mg^{-1} penicillin–streptomycin (Life technologies, CA, USA), and 1% (v/v) non-essential amino acids (NEAA; Life technologies, CA, USA) at 37 °C and 5% CO_2.

Immunocytochemical Staining

Cells were cultured on PA hydrogels with gradient thickness. The cells were fixed with 4% paraformaldehyde for 30 min at room temperature. After The cell membrane was then broken using 0.2% Triton X-100 for 10 minutes at room temperature. Samples were block with 5% bovine serum albumin for 2 h. The slides were then incubated with primary antibodies against activated β1 integrin (1:200; Abcam), Vinculin (1:200; Abcam), YAP (1:200; Abcam), Lamin-A (1:200; Abcam), RUNX2 (1:200; Abcam), Collagen I (1:200; Abcam), Nestin (1:200; Abcam), and NF-68kD (1:200; Abcam) at 4 °C overnight. The slides were incubated with secondary antibody with fluorescence FITC (1:500; Abcam), TRITC (1:500; Abcam) and cy5 (1:200; Abcam) for 2 h at 37 °C. Finally, cell nuclei and F-actin were stained by DAPI (1:1000; Sigma) and phalloidin and were viewed under a LeicaSP8 confocal microscopy system. Quantification of the immunofluorescence signal was performed by measuring average intensity in individual cells according to the ImageJ software manual.

Statistical Analysis.

The data analysis were processed by one-way analysis of variance using Excel and SPSS. Origin was used for plotting. Data were presented as mean ± standard error of mean (SEM), and boxplot format data were presented as median ± min/max, as indicated in the corresponding figure legends. Sample size (n) for each statistical analysis was presented as box plots of all quantifications. Statistical significance was determined by the two-tailed Student's t-test and one-way ANOVA with Tukey's correction, as indicated in the corresponding figure legends. Tukey's posthoc test was used for multiple posthoc comparisons to determine the significance between the groups after one-way analysis of variance (ANOVA). $p < 0.05$ was considered statistically significant. Statistical analysis was carried out using commercial software IBM SPSS Statistics 22.

Finite element simulations

To determine the effect of contact geometry on the contact stiffness, the Finite Element analyses (FEA) was performed using Abaqus/standard[31] (Abaqus 6.14, Dassault Systèmes®). In the simulation, a three-dimensional finite element model has been built, for a given contact area of 4π, we changed the ratio of a/b of the elliptical contact region(as shown in Figure S1 a), wheare a and b are the semi-major and semi-minor axis, respectively. The ECM was assumed to be nearly incompressible (Poisson's ratio $v = 0.49995$) and Young's modulus is taken as $E = 10$ kPa. The displacement boundary was set in the contact area with lower boundary fixed ($u = 0$, $v = 0$ and $w = 0$). We used a uniform mesh grid (element size 0.1 mm) in the contact area, and gradient grid in other areas (element size from 0.1mm to 1.0 mm). The hybrid element-C3D10MH (10-node modified tetrahedron element with hourglass control) was used in the whole model.

Calculation of contact stiffness

The contact stiffness was calculated with $S = \frac{\Delta P}{\Delta h} = C_0 E^* \sqrt{A} \Pi\left(\frac{\sqrt{A}}{t}\right)$, where E^*, A and t are the plane strain modulus of substrate, contact area and substrate thickness of substrate, respectively, E^* is related to Young's modulus (E) and Poisson's ratio (v) of substrate by $E^* = E/\left(1-v^2\right)$, E is measured with indentation tests (Optics11, PIUMA) and tip with radius of 10 μm is used. C_0 is a geometrical factor given by finite element analysis (FEA) considering the contact geometry. Π is a dimensionless function determined via FEA as well.

RRFERENCES

1 Wen, J. *et al.* Interplay of matrix stiffness and protein tethering in stem cell differentiation. *Nat. Mater.* **13**, 979-987, doi:10.1038/nmat4051 (2014).

2 Engler, A., Sen, S., Sweeney, H. & Discher, D. Matrix elasticity directs stem cell lineage specification. *Cell* **126**, 677-689, doi:10.1016/j.cell.2006.06.044 (2006).

3 Wang, S. *et al.* BMSC-derived extracellular matrix better optimizes the microenvironment to support nerve regeneration. *Biomater.* **280**, 121251, doi:10.1016/j.biomaterials.2021.121251 (2022).

4 Bao, M., Xie, J., Piruska, A. & Huck, W. 3D microniches reveal the importance of cell size and shape. *Nat. commun.* **8**, 1962, doi:10.1038/s41467-017-02163-2 (2017).

5 Lee J, Abdeen A A, Zhang D l, Kilian K A.(2013). Directing stem cell fate on hydrogel substrates by controlling cell geometry, matrix mechanics and adhesion ligand composition. *Biomater.*, 34(33), 8140-8. doi:10.1016/j.biomaterials.2013.07.074

6 Johnson, K. L. & Johnson, K. L. *Contact mechanics*. (Cambridge university press, 1987).

7 Pharr, G., Oliver, W. C. & Brotzen, F. On the generality of the relationship among contact stiffness, contact area, and elastic modulus during indentation. *J. Mater. Res.* **7**, 613-617 (1992).

8 Gao, H., Cheng-Hsin, C. & Jin, L. Elastic contact versus indentation modeling of multi-layered materials. *Int. J. Solids Struct.* **29**, 2471-2492 (1992).

9 Kumar, A., Placone, J. & Engler, A. Understanding the extracellular forces that determine cell fate and maintenance. *Development (Cambridge, England)* **144**, 4261-4270, doi:10.1242/dev.158469 (2017).

10 Sen, S., Engler, A. & Discher, D. Matrix strains induced by cells: Computing how far cells can feel. *Cell. Mol. Bioeng.* **2**, 39-48, doi:10.1007/s12195-009-0052-z (2009).

11 Sneddon, I. N. The relation between load and penetration in the axisymmetric Boussinesq problem for a punch of arbitrary profile. *Int. J. Eng. Sci.* **3**, 47-57 (1965).

12 Cao, Y., Ma, D. & Raabe, D. The use of flat punch indentation to determine the viscoelastic properties in the time and frequency domains of a soft layer bonded to a rigid substrate. *Acta Biomater.* **5**, 240-248 (2009).

13 Hadden, W. *et al.* Stem cell migration and mechanotransduction on linear stiffness gradient hydrogels. *Proc. Natl Acad. Sci. USA* **114**, 5647-5652, doi:10.1073/pnas.1618239114 (2017).

14 Leong, W. *et al.* Thickness sensing of hMSCs on collagen gel directs stem cell fate. *Biochem. Biophys. Res. Commun.* **401**, 287-292, doi:10.1016/j.bbrc.2010.09.052 (2010).

15 Huang, D., Bax, N., Buckley, C., Weis, W. & Dunn, A. Vinculin forms a directionally asymmetric catch bond with F-actin. *Science* **357**, 703-706, doi:10.1126/science.aan2556 (2017).

16 Pomp, W. *et al.* Cytoskeletal Anisotropy Controls Geometry and Forces of Adherent Cells. *Phys. Rev. Lett.* **121**, 178101, doi: 10.1103/PhysRevLett.121.178101 (2018).

17 Dupont, S. *et al.* Role of YAP/TAZ in mechanotransduction. *Nature* **474**, 179-183, doi:10.1038/nature10137 (2011).

18 Alisafaei, F., Jokhun, D., Shivashankar, G. & Shenoy, V. Regulation of nuclear architecture, mechanics, and nucleocytoplasmic shuttling of epigenetic factors by cell geometric constraints. *Proc. Natl Acad. Sci. USA* **116**, 13200-13209, doi:10.1073/pnas.1902035116 (2019).

19 Swift, J. *et al.* Nuclear lamin-A scales with tissue stiffness and enhances matrix-directed differentiation. *Science* **341**, 1240104, doi:10.1126/science.1240104 (2013).

20 Ranade, D., Pradhan, R., Jayakrishnan, M., Hegde, S. & Sengupta, K. Lamin A/C and Emerin depletion impacts chromatin organization and dynamics in the interphase nucleus. *BMC Mol. Cell Biol.* **20**, 1-20 (2019).

21 Ohta, Y. *et al.* Cell-matrix interface regulates dormancy in human colon cancer stem cells. *Nature* **608**, 784-794, doi:10.1038/s41586-022-05043-y (2022).

22 Meli, V. *et al.* YAP-mediated mechanotransduction tunes the macrophage inflammatory response. *Sci. Adv.* **6**, doi:10.1126/sciadv.abb8471 (2020).

23 Gandin, A. *et al.* Broadly Applicable Hydrogel Fabrication Procedures Guided by YAP/TAZ-Activity Reveal Stiffness, Adhesiveness, and Nuclear Projected Area as Checkpoints for Mechanosensing. *Adv. Healthc. Mater.* **11**, e2102276, doi:10.1002/adhm.202102276 (2022).

24 Feng, F., Feng, X., Zhang, D., Li, Q. & Yao, L. Matrix Stiffness Induces Pericyte-Fibroblast Transition Through YAP Activation. *Front. Pharmacol.* **12**, 698275, doi:10.3389/fphar.2021.698275 (2021).

25 Jiao, F., Zhao, Y., Sun, Q. & Huo, B. Spreading area and shape regulate the apoptosis and osteogenesis of mesenchymal stem cells on circular and branched micropatterned islands. *J. Biomed. Mater. Res. Part A* **108**, 2080-2089, doi:10.1002/jbm.a.36967 (2020).

26 He, L., Si, G., Huang, J., Samuel, A. & Perrimon, N. Mechanical regulation of stem-cell differentiation by the stretch-activated Piezo channel. *Nature* **555**, 103-106, doi:10.1038/nature25744 (2018).

27 Taniguchi, J. *et al.* A synthetic DNA-binding inhibitor of SOX2 guides human induced pluripotent stem cells to differentiate into mesoderm. *Nucleic Acids Res.* **45**, 9219-9228, doi:10.1093/nar/gkx693 (2017).

28 Cai, P. *et al.* Bio-inspired mechanotactic hybrids for orchestrating traction-mediated epithelial migration. *Adv. Mater.* **28**, 3102-3110 (2016).

29 Barriga, E., Franze, K., Charras, G. & Mayor, R. Tissue stiffening coordinates morphogenesis by triggering collective cell migration *in vivo*. *Nature* **554**, 523-527, doi:10.1038/nature25742 (2018).

30 Tse, J. R., Engler, A. J.. Preparation of hydrogel substrates with tunable mechanical properties. Curr Protoc Cell Biol, null(undefined), Unit 10.16. doi:10.1002/0471143030.cb1016s47 (2010)

31 **ABAQUS** Analysis User's Manual, Version **6.14** (2014)

SUPPLEMENTARY

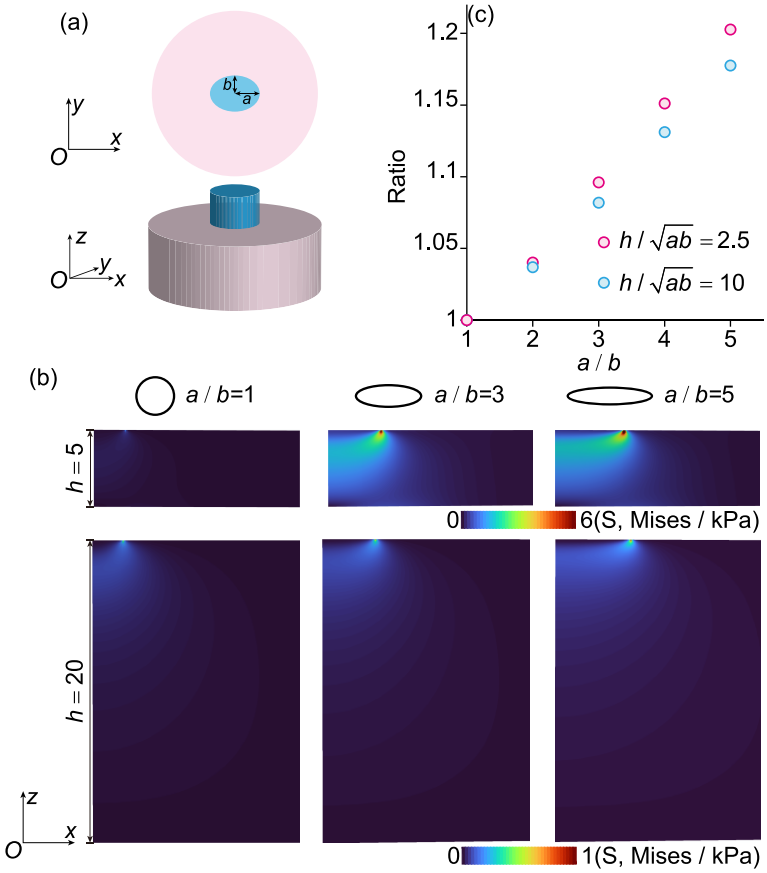

Supplementary Figure S1. Finite element analysis of the effect contact geometry on the contact stiffness (the contact areas are the same for all the cases). **(a)** Finite element model of for the contact with elliptical contact region. **(b)** Contour of stresses in the contact region for different contact geometries and substrate thickness. The results show that the substrate effect will be significant when the substrate is thin and the ratio of a/b is large. **(c)** The ratios of the contact stiffness for different contact geometries with respect to that corresponding to circular contact region.

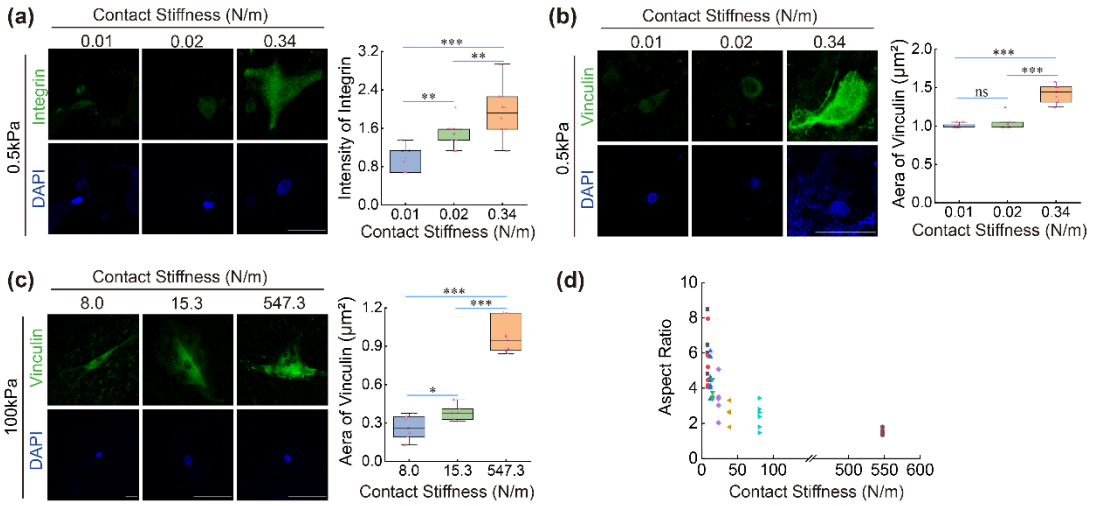

Supplementary Figure S2 Contact stiffness regulates focal adhesion assembly (a) (Left) Representative images of integrin β1 expression and nucleus in MSCs cultured on 0.5 kPa PA hydrogel with different contact stiffness stained by integrin β1 antibody (green) and DAPI (blue), respectively. Scale bar: 50 μm. (Right) The statistical analysis of integrin β1 expression level in MSCs cultured on 0.5 kPa PA hydrogel with different contact stiffness. **(b)** (Left) Representative images of vinculin expression and nucleus in MSCs cultured on 0.5 kPa PA hydrogel with different contact stiffness stained by vinculin antibody (green) and DAPI (blue), respectively. Scale bar: 50 μm. (Right) The statistical analysis of single focal adhesion area in MSCs cultured on 0.5 kPa PA hydrogel with different contact stiffness. **(c)** (Left) Representative images of vinculin expression and nucleus in MSCs cultured on 100 kPa PA hydrogel with different contact stiffness stained by vinculin antibody (green) and DAPI (blue), respectively. Scale bar: 50 μm. (Right) The statistical analysis of single focal adhesion area in MSCs cultured on 100 kPa PA hydrogel with different contact stiffness. **(d)** The statistical analysis of Aspect ratio of MSCs cultured on 100 kPa PA hydrogel with different contact stiffness.*P < 0.05, **P < 0.01, ***P < 0.001.

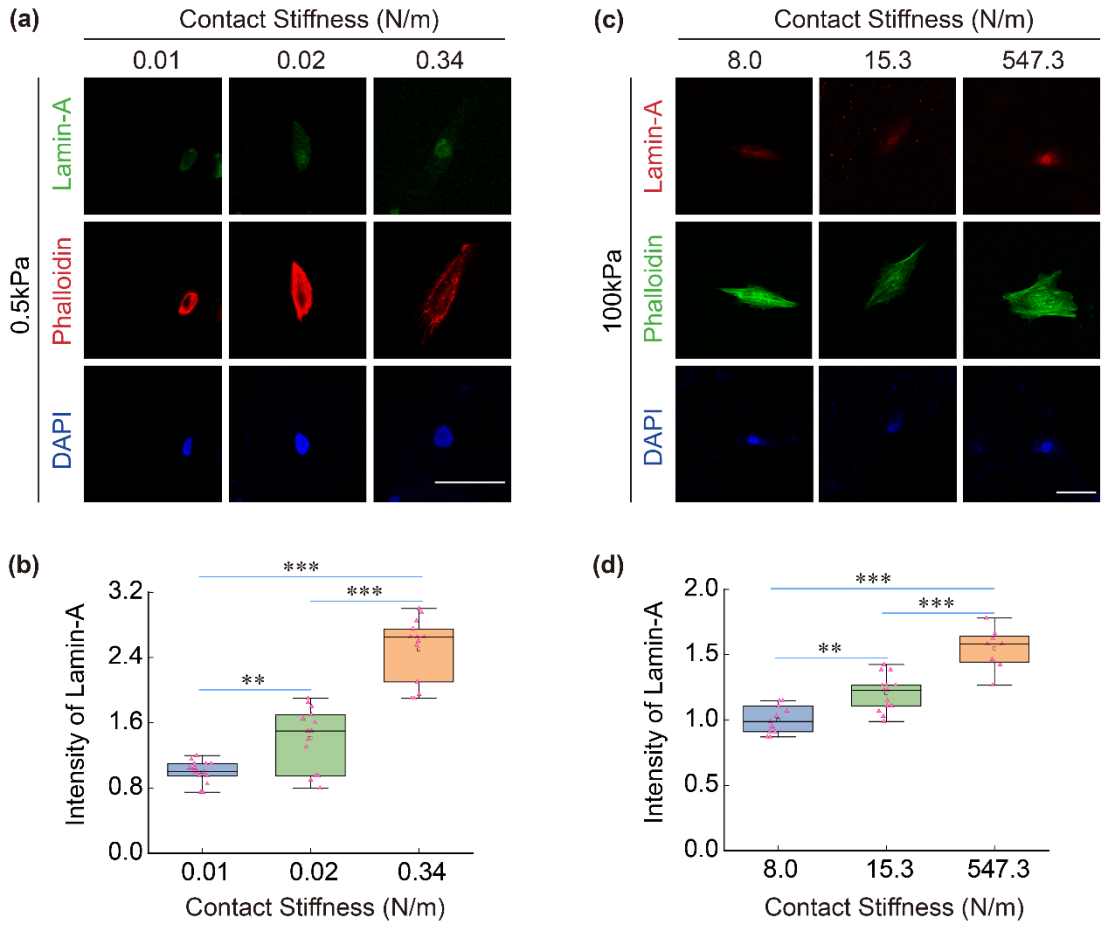

Supplementary Figure S3 Contact stiffness regulates the assembly of nuclear lamina (a) Representative images of Lamin-A, F-actin and nucleus in MSCs cultured on 0.5 kPa PA hydrogel at different contact stiffness stained by Lamin-A antibody (green), phalloidin (red) and DAPI (blue), respectively. Scale bar: 50 μm. **(b)** The statistical analysis of Lamin-A expression level in MSCs cultured on 0.5 kPa PA hydrogel with different contact stiffness in (a). **(c)** Representative images of Lamin-A, F-actin and nucleus in MSCs cultured on 100 kPa PA hydrogel at different contact stiffness stained by Lamin-A antibody (red), phalloidin (green) and DAPI (blue), respectively. Scale bar: 75 μm. **(d)** The statistical analysis of Lamin-A expression level in MSCs cultured on 100 kPa PA hydrogel with different contact stiffness in (c). *P < 0.05, **P < 0.01, ***P < 0.001.

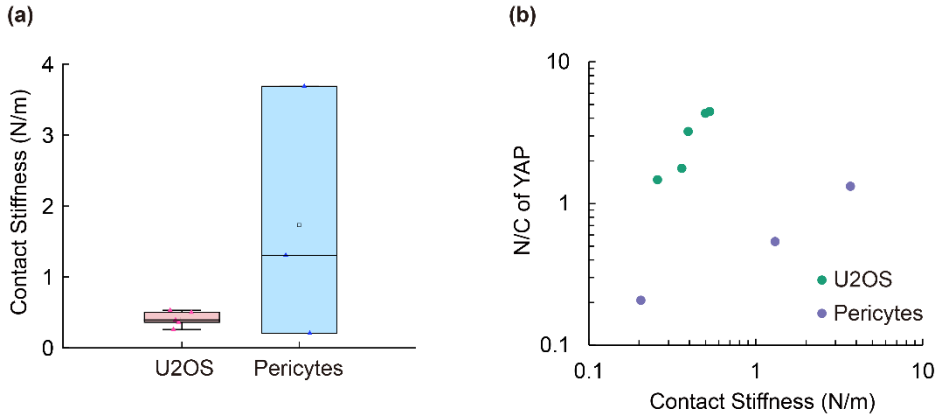

Supplementary Figure S4 A scaling relation between contact stiffness and YAP nuclear/cytoplasmic ratio extracted from data set in the literature. (a) Calculation of the contact stiffness according to the cell spreading area and stiffness of substrate from data set in the literature [23-25]. (b) Scatter plot of YAP nuclear/cytoplasmic ratio at different contact stiffness from data set in the literature.